Chinese Journal of
POLYMER SCIENCE

RESEARCH ARTICLE

https://doi.org/10.1007/s10118-023-2933-3
Chinese J. Polym. Sci. **2023**, *41*, 1250–1260

Promoted Comprehensive Properties of Polyisoprene Rubber with Extremely High Fatigue Resistance Enabled by Oligopeptide Aggregates

Yu He†, Ran Xu†, Rong Zhang, Chang-Cheng Wang, Shi-Qi Li, Jian Cao, Mao-Zhu Tang*, and Yun-Xiang Xu*

College of Polymer Science and Engineering, State Key Laboratory of Polymer Materials Engineering, Sichuan University, Chengdu 610065, China

Electronic Supplementary Information

Abstract For decades, the preparation of polyisoprene rubber that can match the comprehensive properties of natural rubber (NR) has been pursued. While sacrificial bonds have been used to promote the strength and toughness of rubbers, little is known about their effects on fatigue resistance, which is important in dynamic environments. Herein, terminal block and randomly functionalized polyisoprene rubbers tethered with di-alanine, tri-alanine and tetra-alanine were prepared. The results showed that the flow activation energy, aggregates ordering and energy dissipation of the hydrogen-bonded aggregates increase with the elongation of oligopeptide length (*X*A, *X*=2, 3, 4), therefore resulting in enhanced mechanical strength and toughness of corresponding samples. Comparably, the tear strengths are barely affected by oligopeptide lengths in block samples, but promoted from dipeptide to tetrapeptide in random samples, probably due to the well dispersed oligopeptide aggregates. Most importantly, it is found that the tight binding aggregates of oligopeptides are critical for the excellent fatigue resistance, which is absent in polyisoprene and natural rubber. The loose aggregates dissociate and recombine repeatedly under cyclic loading and the tight aggregates keep the network integrated and robust. Interestingly, the largest hysteresis of PIP-4A-V with the longest oligopeptide length give the lowest heat generation, which is contrary to the traditional sacrificial bonds. Overall, the oligopeptide aggregates have repeatable energy dissipation properties and cycle life comparable to or even surpassing those of the linked proteins in NR, resulting in similar tensile strength, fracture toughness, and better fatigue resistance relative to NR. This deep insight on the role of oligopeptide aggregates is very useful for the engineering rubbers served in dynamic environments.

Keywords Polyisoprene; Hydrogen bonding; Oligopeptides; Fatigue resistance

Citation: He, Y.; Xu, R.; Zhang, R.; Wang, C. C.; Li, S. Q.; Cao, J.; Tang, M. Z.; Xu, Y. X. Promoted comprehensive properties of polyisoprene rubber with extremely high fatigue resistance enabled by oligopeptide aggregates. *Chinese J. Polym. Sci.* **2023**, *41*, 1250–1260.

INTRODUCTION

Natural rubber (NR) is a strategically important material, but its resource is restricted by limited planting area and threatened by the disease. The seeking of alternatives of NR is quite critical for national and economic security in this world considering its vast applications. There are more than 2000 kinds of plants that can produce NR worldwide, but the only rubber that has been widely applied is the one extracted from the *Hevea brasiliensis*. Facing this situation, some countries have shifted their direction to bio-based rubber, *i.e.*, rubber synthesized from bio-based raw materials such as starch, glycogen, cellulose, *etc*., or rubber produced from plants such as guayule and dandelion.[1] However, there are still some theoretical problems and technical difficulties, including inferior comprehensive properties, lack of maturity of the processing, high cost of rubber extraction, and difficulty of large-scale industrialization. Therefore, polyisoprene rubber with highly *cis*-1,4 content is still the most promising alternative to replace NR because of its similar chemical composition and stereo configuration.

However, even with high stereoregularity, polyisoprene rubber exhibits only 70%–80% of the elastic modulus, tensile strength and crack extension resistance of NR.[2] One of the most important methods for reinforcing rubber is based on the introduction of sacrificial bonds to effectively improve the strength and fracture toughness of the rubber.[3,4,5] Sacrificial bonds are defined as bonds that rupture prior to the broken of main structural link.[6] Once the sacrificial bond is broken, the hidden length will be released, consuming a large amount of mechanical energy. The presence of sacrificial bonds gives the material high strength and high fracture toughness. For example, Gold *et al*. developed a dual-network elastomer which consists of covalently cross-linked polybutadiene with a hydrogen-bonding network formed by

* Corresponding authors, E-mail: mztang@scu.edu.cn (M.Z.T.)
E-mail: yxxu@scu.edu.cn (Y.X.X.)
† These authors contributed equally to this work.
Received November 15, 2022; Accepted December 19, 2022; Published online February 21, 2023

the association of urazole groups randomly attached to the polybutadiene backbone, conferring increased toughness.[7] Zhang *et al*. introduced weaker multiple hydrogen bonds and stronger Zn-triazole coordination bonds into a *cis*-1,4-polyisoprene matrix and prepared elastomers with high tensile strength and toughness.[8] However, the reversible dissociation/association characteristics of these sacrificial bonds will also deteriorate the resilience of rubber, and increase the hysteresis and heat accumulation under dynamic loading, thus reducing the fatigue life of the rubber and making it difficult to use in dynamic environments.[4] That means the introduction of sacrificial bonds may achieve enhanced strengthening and toughening of rubber at the expense of fatigue life. In fact, the working condition of NR products, such as tires, conveyor belts, seals, shock absorbers, *etc*., is mainly subjected to long-term cyclical loads. Thus, the ability to maintain their mechanical properties under cyclic forces is highly demanded. Therefore, it remains an important challenge to obtain rubber materials with high strength, high toughness and high fatigue resistance simultaneously through sacrificial bonding strategies.

Nature is the source of wisdom. It is generally believed that the existence of "none rubber components" is the reason for the superior properties of NR.[9,10] Among them, proteins are the most representative non-rubber components, including linked proteins and free proteins, which are bound to the ω-terminus of NR *via* hydrogen bonds or free in natural rubber latex, respectively.[11–13] It is now generally accepted that the non-rubber components improve the mechanical properties of NR by enhancing the SIC behavior.[14–17] However, Huang *et al*. demonstrated that the physical linkage network formed by the linked protein could be used as a sacrificial network, which could lead to high strength, high toughness and fatigue properties of vulcanized NR.[18] After compression cycles of 3×10^6 times, 94% of initial sacrificial bonds of linked protein are still maintained, while only 19% of weak bonds could be maintained after the removal of the linked protein. Moreover, Liao *et al*. showed that adding the proper amount of protein to deproteinated NR can promote the formation of sulfide network, increase the cross-linking density and make the molecular chains movement more difficult.[19] The corresponding frictional behavior generates less heat, thus reducing the heat generation.[19] Therefore, it is expected that the mechanical and fatigue resistance properties could be improved simultaneously by mimicking the structure and function of linked proteins of NR. However, the composition, structure and function mechanism of linked proteins are quite complex, which make the structural and functional mimicking in synthetic rubber very challenging.

As well known, α-helix or β-sheet structures are essential components of proteins, which could be harvested from self-assembly of short amino acid.[20] For example, oligo-alanines $(ala)_n$ are hard segments of spider silk and form highly ordered antiparallel β-sheet nanocrystals, contributing to the extremely high tensile strength and toughness.[21] When the oligo-alanines are introduced into polyisoprene matrix, the oligopeptides self-assemble into aggregates with different ordering depending on the polymer sequence or dangling chain lengths, functioning as nanofillers and sacrificial bonds simultaneously.[22–23] It is a straightforward thought that oligo-alanines with different lengths could be introduced into polyisoprene chain end to mimicking the function of linked protein, by which the binding strength of oligopeptide could be tuned gradually and proper structures of sacrificial bonds beneficial for both mechanical strength and fatigue resistance may be found. In detail, oligo-alanines $(ala)_n$ (n=2, 3, 4) functionalized polyisoprene with block and random sequences were prepared, which are attached with $(CH_2)_7$ spacer to increase the spatial freedom of oligopeptide self-assembly.[24] Only a very short polar block is attached on the terminal of polyisoprene and the content of attached oligopeptides is about 2 wt%, comparable to the protein content in NR. Therefore, the assembly of oligopeptides on block copolymers are expected to mimic the structures of linked proteins. While randomly functionalized polyisoprenes are designed to investigate the influence of oligopeptide distribution, and potentially give more synthetic structures available other than those biomimicking ones. It is found that tight and loose oligopeptide aggregates exist in all functionalized polyisoprenes, and the number of tight aggregates increase with the length of the oligopeptide (Scheme 1). As results, the tensile strength, fracture toughness and fatigue resistance of the decorated polyisoprene rubbers are comparable or superior to those of NR along with the increase of oligopeptide lengths. Among them, the fatigue resistance and heat accumulation properties of PIP-4A-V were best, although their hystereses are the highest, which become even bigger after five hundred thousand of cyclic loading.

EXPERIMENTAL

Materials

Neodymium neodecanoate [$Nd(VA)_3$] was purchased from Meryer and used as a hexane solution (solid content: 0.069 g/mL). Triisobutylaluminium [$Al(i\text{-}Bu)_3$] (1.1 mol/L solution in toluene) and diisobutylaluminum Chloride [$Al(i\text{-}Bu)_2Cl$] (0.8 mol/L solution in heptane) were purchased from Acros Chemical. Isoprene was purchased from Alfa, refluxed over CaH_2 for 2 h and distilled prior to use. Hexane and tetrahydrofuran were refluxed over sodium/diphenylketone under nitrogen and then distilled before use. Other chemicals, unless otherwise specified, were purchased from Aldrich and used as received. Boc-*X*Ala-OCH_2Ph (X=2, 3, 4) and 8-methylenedec-9-en-1-ol were prepared according to reported procedures.[25,26]

Sample Preparation

Synthesis of PIP-BOH

All the manipulations were performed under a dry nitrogen atmosphere. Step 1: Synthesis of Al-IP. To a cooled (−78 °C) hexane solution of $Al(i\text{-}Bu)_2H$ (49.5 mL, 1 mol/L in hexane) was added to 8-methylenedec-9-en-1-ol (OH-IP, 8.33 g, 49.54 mmol). The reaction was allowed to warm to room temperature and stirred overnight. After filtering the supernatant, the solution is stored at −25 °C for next reaction. The solid content of Al-IP solution is 57.25 mg/mL. Step 2: $Nd(VA)_3$ (134.6 μL, 0.053 mmol), Al-IP (7.2 mL,1.056 mmol) and $Al(i\text{-}Bu)_3$ (462 μL, 0.528 mmol) were injected into a glass tube with septum *via* syringes and aged at 50 °C for 10 min, then $Al(i\text{-}Bu)_2Cl$ (66 μL, 0.053 mmol) was injected and reacted for 1 h before use. Isoprene (3 mol/L in hexane, 0.238 mol, 71 mL) was placed in an oxygen and moisture-free ampule capped with a rubber. After the monomer solution was brought to a desired temperature, the preformed

https://doi.org/10.1007/s10118-023-2933-3

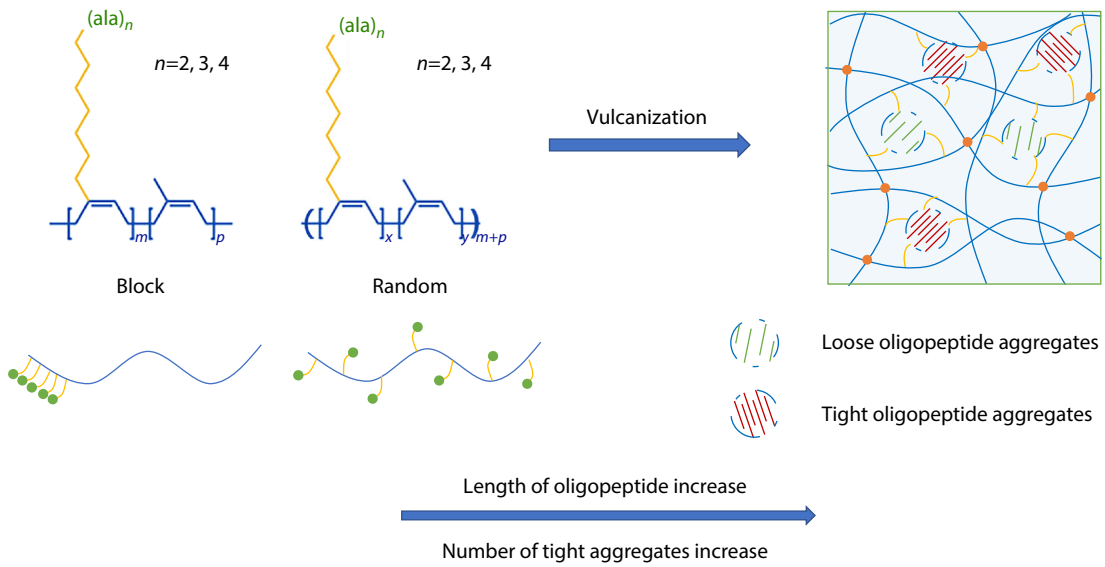

Scheme 1 Proposed model of the network in oligopeptide functionalized polyisoprene.

catalyst solution was added. Polymerizations were carried out at 50 °C for 4 h and quenched by adding 2.0 mL of acidified ethanol. The polymer was washed with acidified water and ethanol respectively, and then dried in vacuum at 40 °C to obtain a colorless solid (13.6 g, 84.5%). The polymer yield was determined by gravimetric analysis. The NMR spectrum of PIP-BOH is shown in Fig. S1 (in the electronic supplementary information, ESI).

Synthesis of PIP-ROH

All the manipulations were performed under a dry nitrogen atmosphere. $Nd(VA)_3$ (278 μL, 0.044 mmol), isoprene (0.5 mol/L in hexane, 1.76 mmol, 3.52 mL) and $Al(i\text{-}Bu)_3$ (800 μL, 0.76 mmol) were injected into a glass tube with septum *via* syringes and aged at 50 °C for 10 min, then $Al(i\text{-}Bu)_2Cl$ (110 μL, 0.088 mmol) was injected and reacted for 1 h before use. Isoprene (3 mol/L in hexane, 0.33 mol, 99 mL) and Al-IP (8.3 mL, 1.54 mmol) were placed in an oxygen and moisture-free ampule capped with a rubber septum. After the monomer solution was brought to a desired temperature, the preformed catalyst solution was added. Polymerizations were carried out at 50 °C for 6 h and quenched by adding 5.0 mL of acidified ethanol. The polymer was washed with acidified water and ethanol respectively, and then dried in vacuum at 40 °C to obtain a colorless solid (18.6 g, 83.0%). The polymer yield was determined by gravimetric analysis. The NMR spectrum of PIP-ROH is shown in Fig. S2 (in ESI).

Synthesis of PIP-BXA (X=2, 3, 4)

Step 1. The preparation of *X*Ala-OCH_2Ph. Trifluoroacetic acid (TFA) was slowly added into a stirred suspension of Boc-2Ala-OCH_2Ph (1.283 mg, 3.66 mmol) in dichloromethane (5 mL), which was synthesized according to the reported procedures.[25] The mixture was stirred at room temperature overnight. Subsequently, the resulting mixture was concentrated by rotary evaporation to obtain 2Ala-OCH_2Ph in essentially quantitative yield. The reaction product was used directly in the next step without further purification. 3Ala-OCH_2Ph and 4Ala-OCH_2Ph were obtained by a similar synthesis procedure.

Step 2. The preparation of PIP-B-DSC. PIP-BOH (12 g, M_n=6.57×10^5 g/mol) in 1000 mL of dry THF was slowly added into a stirred solution of *N*,*N*′-disuccinimidyl carbonate (48 g, 187.37 mmol) and 4-dimethylaminopyridine (24 g, 19.64 mmol) in DMF (720 mL) and THF (3200 mL) at room temperature and proceeded for 8 h. After evaporated, the mixture was poured into acetonitrile. The precipitate was collected and dried to afford a gray elastomer (11.2 g, 93.3%). The percent of hydroxyl decorated by *N*,*N*′-disuccinimidyl carbonate is 99.7%, which is calculated from NMR, as is shown in Fig. S3 (in ESI).

Step 3. The synthesis of PIP-B*X*A. PIP-B-DSC (11.2 g, obtained in the step 2) in 1000 mL of dry THF was slowly added into a stirred solution of 2Ala-OCH_2Ph (1.14 mmol, obtained in the step 1, dissolved in 60 mL of DMSO) and diisopropylethylamine (DIEA, 70 mL) in THF (3000 mL) and water (20 mL) at room temperature and stirred for 10 h. After evaporated, the mixture was poured into water. The precipitate was collected and dried to afford a gray elastomer (10.8 g, 96.4%). PIP-B3A and PIP-B4A were obtained by a similar synthesis procedure. The percent of carbonate replaced by 2Ala-OCH_2Ph, 3Ala-OCH_2Ph and 4Ala-OCH_2Ph are all about 100%, which is calculated from NMR, as is shown in Figs. S4–S6 (in ESI).

Synthesis of PIP-RXA

Step 1. The preparation of PIP-R-DSC. PIP-ROH (12 g, M_n=6.32×10^5 g/mol) in 1000 mL of dry THF was slowly added into a stirred solution of *N*,*N*′-disuccinimidyl carbonate (48 g, 187.37 mmol) and 4-dimethylaminopyridine (24 g, 19.64 mmol) in DMF (720 mL) and THF (3200 mL) at room temperature and proceeded for 8 h. After evaporated, the mixture was poured into acetonitrile. The precipitate was collected and dried to afford a gray elastomer (11.4 g, 95%). The percent of hydroxyl decorated by *N*,*N*′-disuccinimidyl carbonate is 99.7%, which is calculated from NMR, as is shown in Fig. S7 (in ESI).

Step 2. The synthesis of PIP-RXA. PIP-R-DSC (11.4 g, obtained in step 2) in 1000 mL of dry THF was slowly added into a stirred solution of 2Ala-OCH_2Ph (1.14 mmol, obtained in step 1, dissolved in 60 mL of DMSO) and diisopropylethylamine (DIEA, 70 mL) in THF (3000 mL) and water (20 mL) at room

https://doi.org/10.1007/s10118-023-2933-3

temperature and stirred for 8 h. After evaporated, the mixture was poured into water. The precipitate was collected and dried to afford a gray elastomer (11.1 g, 97.4%). The percent of carbonate replaced by 2Ala-OCH_2Ph, 3Ala-OCH_2Ph and 4Ala-OCH_2Ph are all about 100%, which is calculated from NMR, as is shown in Figs. S8–S10 (in ESI).

Preparation of PIP-XA-V (X=2, 3, 4)

The vulcanized rubbers (PIP-*X*A-V) were compounded with rubber ingredients in an open double roller mill. Among them, rubbers were mixed with zinc oxide 5 and stearic acid 2, and then mixed with antioxidant 4020 1 and antiaging agent RD. Finally, the rubber was mixed with sulfurizing promoter CZ 1 and sulfur 2 (relative to 100 parts of PIP-B*X*A-V). After mixing, the sample was stored for 16–24 h, and then subjected to a hot pressing for 21 min at 143 °C and a cold pressing for 10 min in a rubber processing analyzer (RPA).

Characterizations

^{1}H-NMR spectrometer (Bruker AV III HD 400 MHz), GPC (HLC-8320GPC, TOSOH), FTIR spectrometer (Perkin Elmer LX10-8873), DSC (TA Q200), DMA (TA Q800), AFM (Seiko SPI 4000), XRD (Rigaku Ultima IV), TGA (TG209F1), ultramicrotome (Leica EMUC6/FC6), TEM (FEI Tecnai G2F20S-TWIN), Universal testing machine (INSTRON 5996), Fatigue resistance test (MTS 647), Vulcameter (RPA8000), WAXD (beamline BL16B1), MTS test (MTS Series 647). More details of material characterization are given in ESI.

RESULTS AND DISCUSSION

Design, Synthesis and Characterization of Polyisoprene Rubbers

First, two hydroxyl-functionalized polyisoprenes PIP-BOH and PIP-ROH with different sequences were synthesized by changing the addition order of polar monomer and isoprene, as shown in Scheme 2. PIP-BOH and PIP-ROH represent polyisoprene derivatives with block and random distribution of hydroxy groups, respectively. PIP-BOH was synthesized by sequential addition of isoprene after the complete reaction of OH-IP. It is shown that the peak of OH-IP disappeared completely after 1 h (Fig. S11 in ESI), and then isoprene was added to continue the reaction to form block copolymer PIP-BOH. PIP-ROH was synthesized by mixing OH-IP with isoprene monomer directly and then adding aged catalyst. Both PIP-BOH and PIP-ROH possess similar molecular weight, *cis* content and hydroxyl contents, as shown in Table 1.

In the second step, a multi network of functionalized polyisoprene was constructed by grafting *α*-alanine oligopeptides and sulfur vulcanization as shown in Scheme 2. The intermolecular hydrogen bonding of polyisoprene derivatives was regulated by grafting different length of oligo-

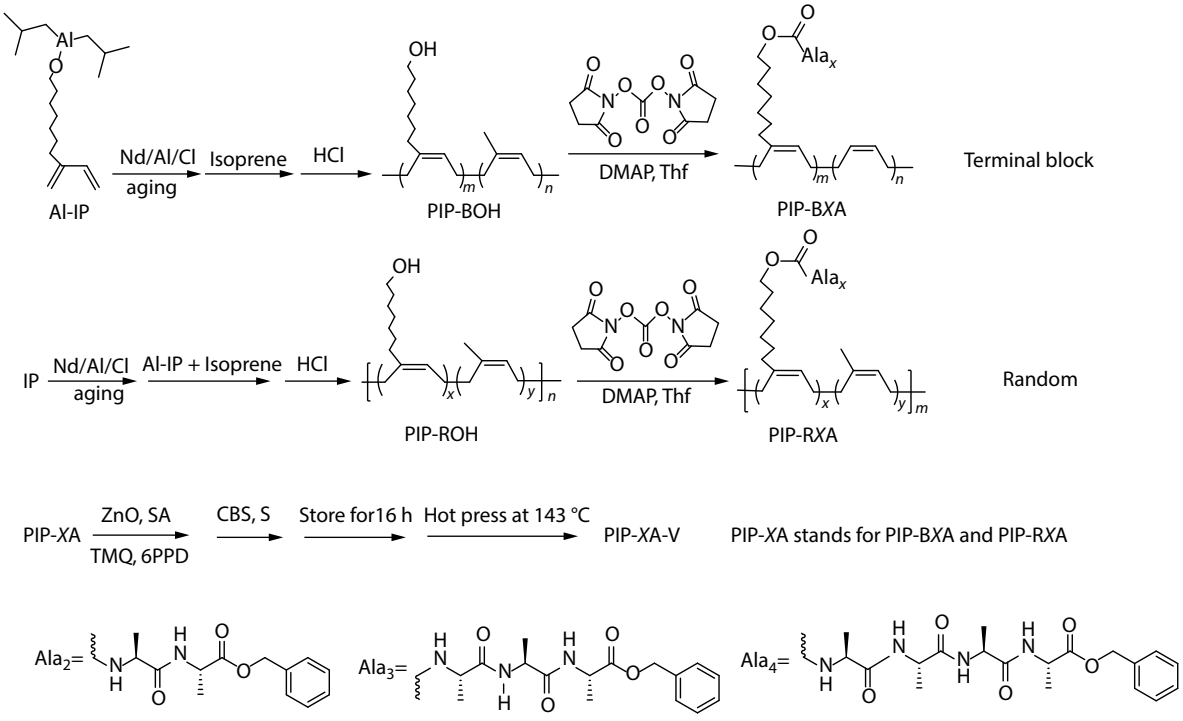

Scheme 2 Synthetic route to functionalized polyisoprene.

Table 1 Characteristics of PIP-BOH and PIP-ROH.

Run [a]	Al-IP/Nd	IP/Nd	IP/OH-IP [b]	*cis*1,4 [b] (%)	M_n [c] (×10^{-4})	PDI [c]
PIP-BOH	40	9000	193/1	96.6	65.7	2.21
PIP-ROH	40	9000	184/1	96.3	63.2	2.35

[a] Polymerization conditions: [Al(*i*-Bu)$_3$]/[Nd(VA)$_3$]=40 (molar ratio), [Al(*i*-Bu)$_2$Cl]/ [Nd(VA)$_3$]=2 (molar ratio), [IP]=3 mol/L, *t*=4 h, *T*=50 °C; [b] Structural unit ratio of copolymer calculated from ^{1}H-NMR (400 MHz, in $CDCl_3$); [c] Determined by GPC (THF, PS calibration).

https://doi.org/10.1007/s10118-023-2933-3

alanines. The successful synthesis of PIP-*X*A (PIP-B*X*A and PIP-R*X*A (*X*=2, 3, 4), *X*A refers to oligopeptide consisting of *X* ala) was demonstrated by ^{1}H-NMR spectra. The hydroxyl peaks of PIP-OH (including PIP-BOH and PIP-ROH) disappear completely and new characteristic peaks of oligopeptides appear, indicating that oligopeptides were successfully grafted (Figs. S1–S10 in ESI). Then PIP-*X*A samples were vulcanized by sulfur, generating PIP-*X*A-V which include PIP-B*X*A-V and PIP-R*X*A-V, respectively. Although polyisoprene rubbers have been modified by oligopeptides, their glass transition temperatures (T_gs) are only slightly changed (Fig. S12 in ESI). The relatively small amounts of oligopeptides do not affect the segmental motion of polymer chain significantly, which is beneficial to keep the original elasticity of rubbers. Further thermogravimetric analysis reveals that the initial decomposition temperatures of both PIP-*X*A and PIP-*X*A-V in nitrogen are higher than 310 °C (Fig. S13 in ESI). The results indicate that these elastomers have excellent thermal stability and meet industrial requirements.

Oligopeptide Interactions of PIP-*X*A

In order to probe the oligopeptide interaction in the bulk state, Fourier transform infrared (FTIR) spectra of PIP-*X*A samples were acquired with PIP as the control sample. The characteristic bands of the *β*-sheet structure at 1538, 1632 and 1706 cm^{-1} appear in PIP-*X*A, and their intensity increase with the elongation of oligopeptide length (Fig. 1a).[27] In comparison, the FTIR of PIP shows characteristic peaks of polyisoprene only in the low frequency range. This verifies our conjecture that oligopeptides with different lengths form *β*-sheet structures with different ordering in polyisoprene matrix.

To quantitatively characterize the effect of oligopeptide length and distribution on the binding strength, frequency-dependent rheological experiments were performed in a range of temperature from 283.15 K to 363.15 K. It is worth noting that the *G*′ values follow the time-temperature superposition principle quite well and collapse onto a master curve by applying horizontal and vertical shift factors on the moduli curves at different temperatures (Fig. S14 in ESI). The horizontal shift factors (a_T) as a function of temperature can be fitted using the Arrhenius equations. With T_{ref}=283.15 K, the activation energy of viscoelasticity (E_a) was shown in Figs. 1(b) and 1(c) for PIP-B*X*A and PIP-R*X*A, respectively. It can be seen that the binding energy of the samples increases with the introduction and increasing length of the oligopeptide. As comparison, the flow activation energy of PIP is close to that of PIP-B2A, indicating that dipeptide at the polymer terminal did not confine the chain movement significantly. For NR, the value is between those of PIP-2A and PIP-3A, demonstrating the tunable binding strength of oligopeptide aggregates. Among them, PIP-B4A and PIP-R4A possess the highest activation energy of 109.6 and 110.4 kJ/mol, respectively.

Mechanical Properties and Energy Dissipation of PIP-*X*A-V

The stress-strain curves of PIP-*X*A are shown in Figs. 2(a) and 2(b). And the values of fracture toughness which is defined as the area under the stress-strain curves of PIP-*X*A are shown in Fig. 2(c). The unmodified PIP has low tensile strength and toughness, while these properties of PIP-*X*A are significantly improved with the introduction of oligopeptides and the increase of oligopeptide length. Especially, the tensile strengths of PIP-B4A and PIP-R4A reached up to 8 and 12 MPa. It is worth noting that the tensile strength of neat PIP-B4A is similar to that of green NR.

The stress-strain curves of vulcanized PIP-*X*A-V are shown in Figs. 2(d) and 2(e). The tensile strength of the sample increased significantly after vulcanization, with PIP-B4A-V and PIP-R4A-V having large tensile strengths (23.9 and 24.6 MPa), which were similar with NR-V and much higher than those of PIP-V. From another aspect, the tensile modulus (tensile stress

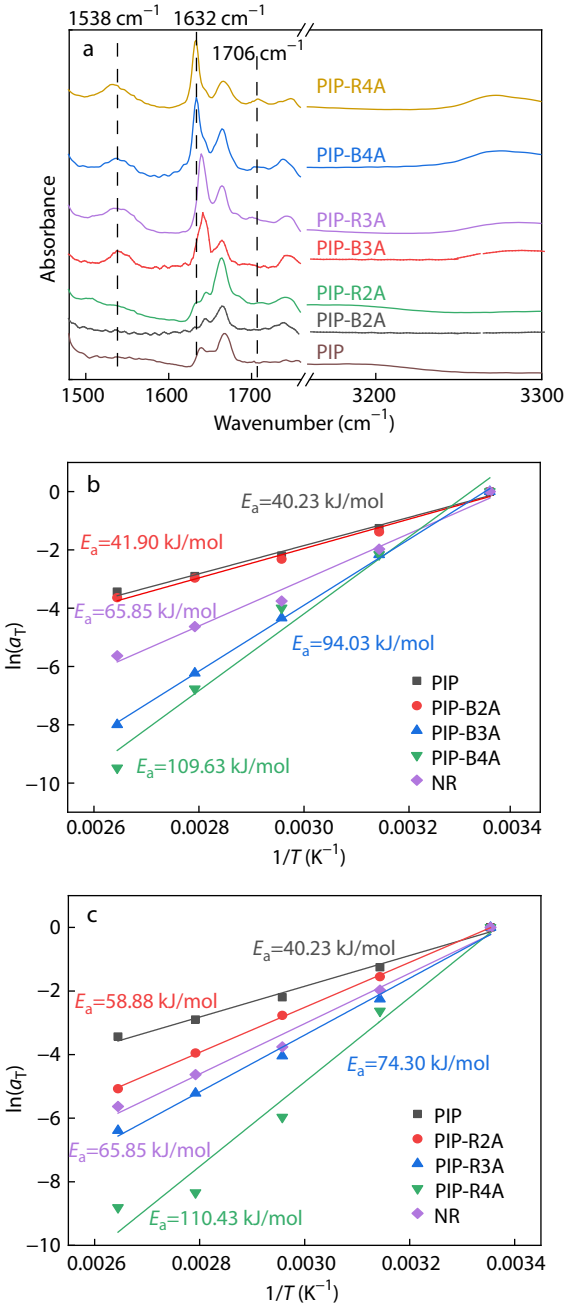

Fig. 1 (a) FTIR spectra of PIP and PIP-*X*A (*X*=2, 3, 4). (b, c) Arrhenius plot of the horizontal shift factor a_T with a reference temperature of 283.15 K of PIP, PIP-B*X*A, PIP-R*X*A and NR.

https://doi.org/10.1007/s10118-023-2933-3

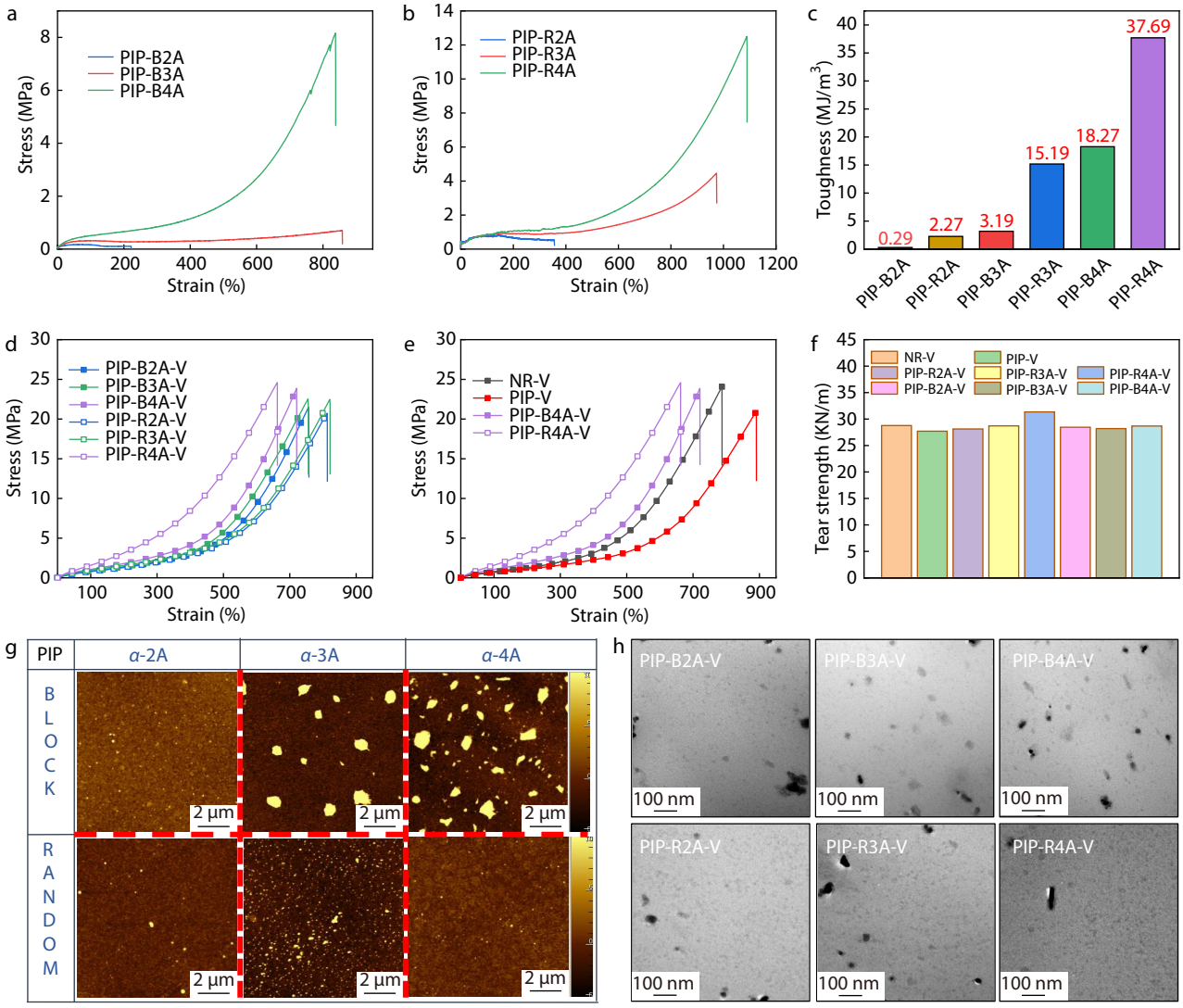

Fig. 2 Mechanical properties of PIP-*X*A and PIP-*X*A-V. (a, b) Representative stress-strain curves of PIP-*X*A with increasing oligopeptide length; (c) Fracture toughness for PIP-*X*A; (d, e) Representative stress-strain curves of PIP-*X*A-V; (f) Tear strength of NR-V, PIP-V and PIP-*X*A-V; (g) AFM height maps of PIP-*X*A; (h) TEM micrographs of PIP-*X*A-V (*X*=2, 3, 4).

at 100% strain, similarly hereinafter) of PIP-*X*A-V is significantly improved. Among them, PIP-R4A-V has the highest modulus, which is 2 times that of NR-V and similar to NR reinforced with carbon black.[28] As shown in Table S1 (in ESI), the oligopeptide increased the crosslink density of the vulcanized PIP-V, thus increasing the tensile strength. However, the tensile strength of PIP-R3A-V with lower crosslink density is 2 MPa higher than that of PIP-R2A-V. This indicated that the high modulus and high strength of PIP-*X*A-V are not only related to the increase of crosslinking density, but also to the binding strength of oligopeptides aggregates. As the binding energy of the aggregates increases, greater mechanical forces are required to cause the dissociation of the sacrificial bonds, thus increasing the strength and toughness of the samples. Meanwhile, the modulus of rubbers varies considerably with the distribution of oligopeptides, which is due to the different aggregation status of oligopeptides that can act as nanofillers. The amplification effect of random distribution structure on modulus is more obvious than that of block structure.

The tear strength, as one of the important mechanical properties of engineering rubber, has also been studied as shown in Fig. 2(f). It is not difficult to find that the tear strength of modified polyisoprene is similar to that of PIP-V, except for PIP-R4A-V which has improved tear strength. These results are related to the position and strength of oligopeptides. Fig. 2(g) shows the morphology of oligopeptide aggregates in thin film samples (PIP-*X*A) by atomic force microscopy (AFM). Oligopeptide aggregates become larger with increasing length for block samples. PIP-B4A forms larger aggregates partially in the form of bands, which were uniformly dispersed in the matrix. However, PIP-R4A shows a homogeneous morphology with small and contiguous aggregates. This is consistent with the morphology of PIP-*X*A-V obtained by the transmission electron microscopy (TEM) experiment, as shown in Fig. 2(h). Therefore, it can be concluded that uniformly sized and distributed oligopeptide aggregates are more conducive to hinder crack expansion and improve the

https://doi.org/10.1007/s10118-023-2933-3

tear strength.

It is expected that the oligopeptide aggregates, featured by hydrogen bond interactions, can be preferentially oriented or broken during deformation to dissipate energy.[29,30] In order to explore the influence of the energy dissipation caused by the length and distribution of oligopeptides, cyclic tensile tests were performed under different strains. As shown in Fig. 3(a), the hysteresis loss of PIP-V without the introduction of oligopeptides is obviously the lowest under low strain cycles, which is basically due to the loss caused by the friction between molecular chains. In contrast, the hysteresis loss increases with the elongation of the oligopeptide length (Fig. 3b). These phenomena indicate that the hydrogen bonds of oligopeptides effectively dissipate energy during tensile process. Block oligopeptide network has lower hysteresis loops than random oligopeptide network during stretching. The

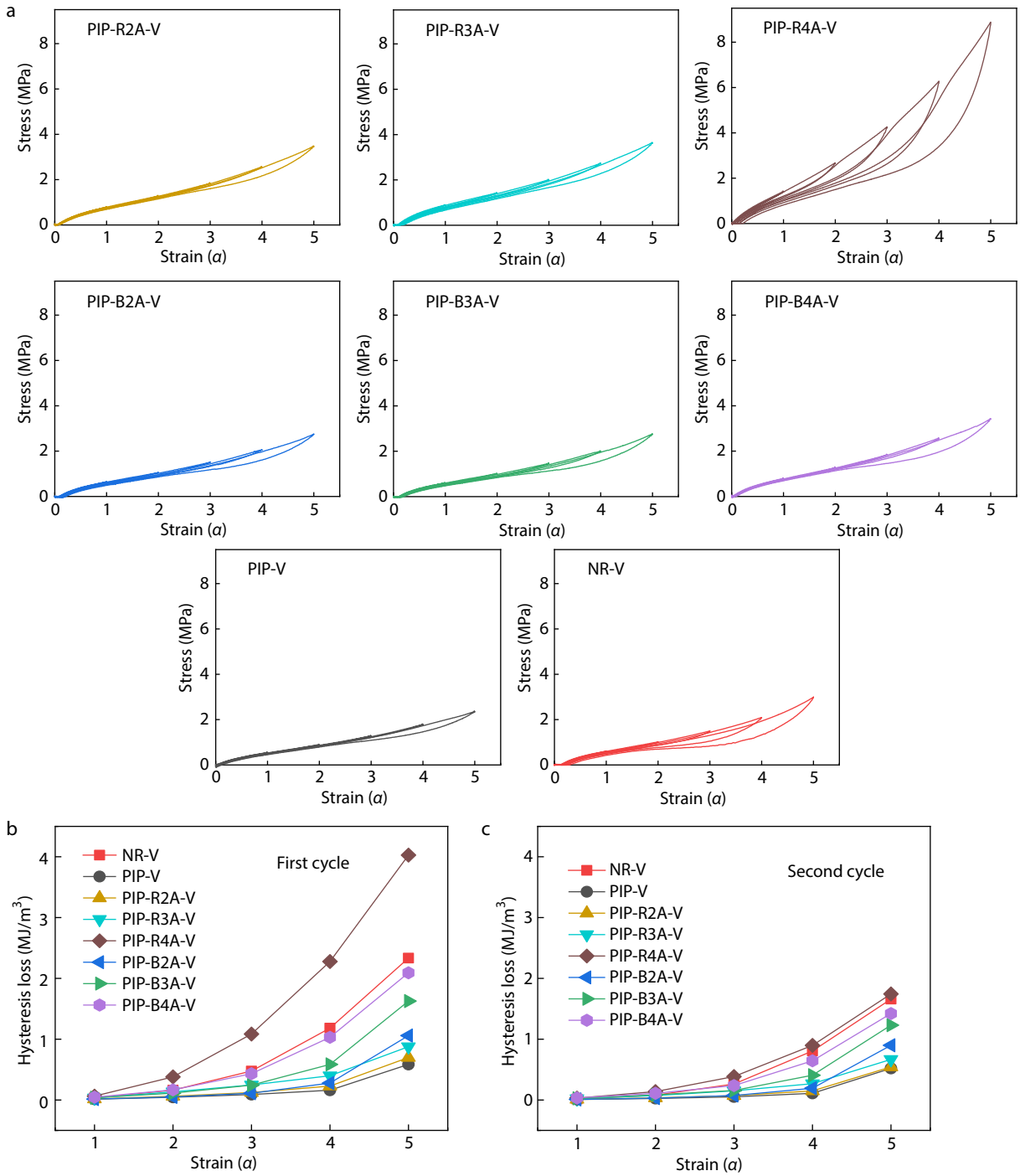

Fig. 3 Energy dissipation during the tensile cycle. (a) Cyclic stress-strain curves of PIP-V, NR-V and PIP-*X*A-V; (b) Hysteresis loss of the first tensile cycle and (c) the second tensile cycle of PIP-V, NR-V and PIP-*X*A-V.

https://doi.org/10.1007/s10118-023-2933-3

reason is that randomly distributed oligopeptide network is more homogeneous than that of block one, and therefore energy is more easily dissipated. In the second cycle shown in the Fig. 3(c), PIP-R4A-V and PIP-B4A-V exhibit closer hysteresis losses, indicating that the consumed hydrogen bonds are not repaired in time.

Dynamic Dissociation and Recombination of Oligopeptide Aggregates in PIP-*X*A-V

To analyze the changes of oligopeptide aggregates under stretching conditions from a microscopic aspect, analysis of wide-angle X-ray diffraction (WAXD) patterns was carried out. The diffraction peaks with 2θ of 10°–19° can be decomposed into an amorphous peak and several crystalline peaks mainly from (200), (201) and (120) planes belonging to SIC of polyisoprene. The diffraction peaks with *d* spacing of 3.02–3.05 Å and 3.34–3.55 Å are ascribed to the hydrogen spacing in the β-sheet structure and extended chain structure, respectively, which is consistent with XRD results (Fig. S15 in ESI). As shown in Fig. 4, all samples show SIC peaks during stretching and hydrogen bonding peaks with *d* spacing of 3.02–3.05 Å and 3.34–3.55 Å. And PIP-3A-V and PIP-4A-V show higher intensity of hydrogen bonding peaks compared to PIP-2A-V, indicating that the ordering of oligopeptide aggregates was greater as the oligopeptide length increased, which enhances the mechanical properties of PIP-*X*A-V.

During stretching and retraction, the diffraction peaks of PIP-*X*A-V corresponding to extended chain structure showed a left-then-right transition, indicating that the extended chain structure became loose and then dense during the cycle. This part of the aggregates can be called loose aggregates, which did not dissociate completely during the deformation process, but only showed changes in the hydrogen bond spacing and dissipated part of the energy. However, the hydrogen spacing of 3.02–3.05 Å belonging to the β-sheet structure did not change significantly during stretching and retraction. These peaks can be referred to as tight aggregates, and their intensity changed irregularly, indicating that one part of these aggregates continuously dissociated and reformed dur-

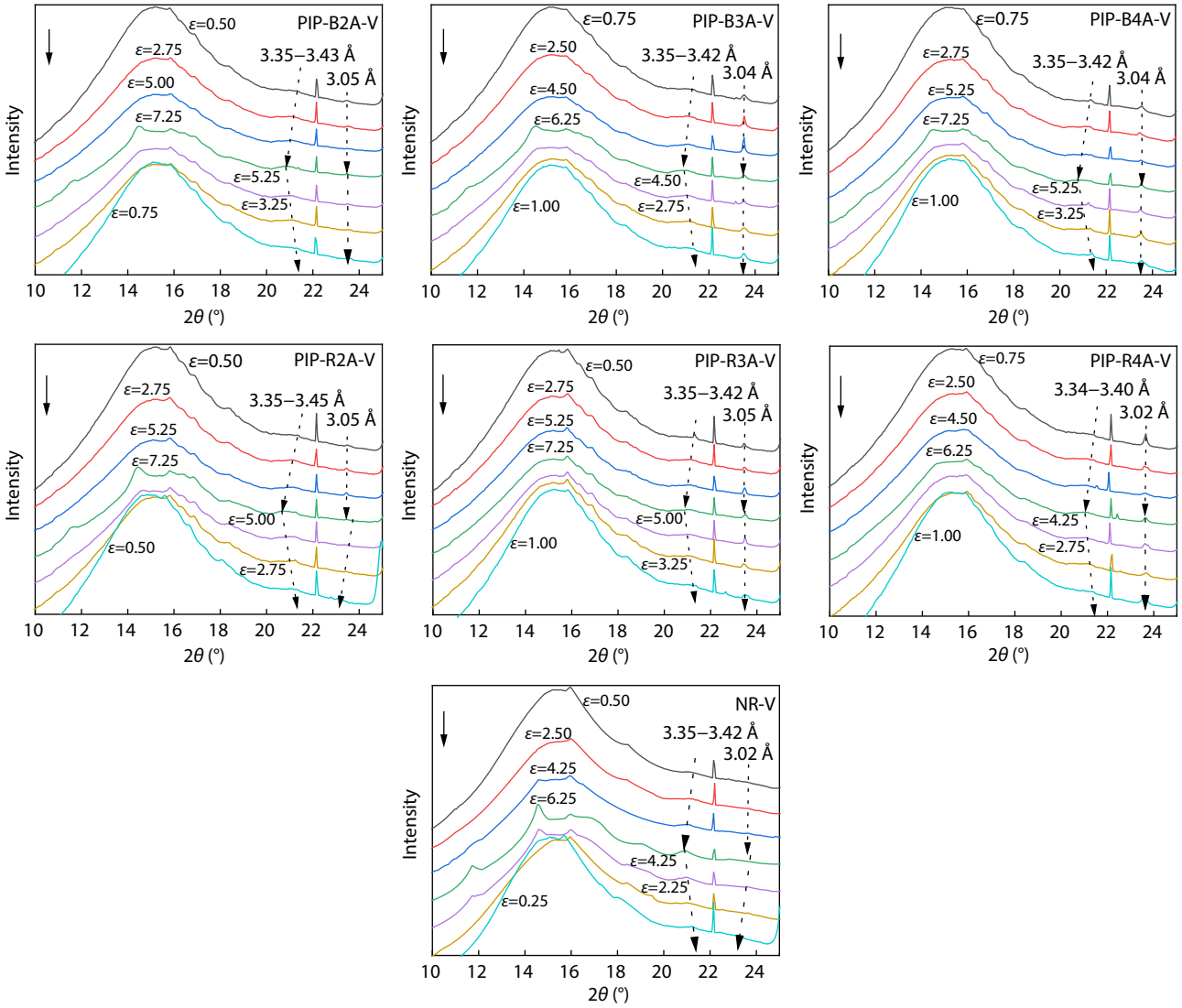

Fig. 4 Variation of β-sheet structure with strain for PIP-*X*A-V and NR-V (The direction of the arrow indicates that the strain increases and then decreases).

https://doi.org/10.1007/s10118-023-2933-3

ing the deformation process and dissipated a certain amount of energy, while the other part kept its structure intact and ensured the integrity of the network to some extent. It can be seen that natural rubber also has tight and loose aggregates and its trend under dynamic loading is similar to that of PIP-*X*A-V. However, the signals of tight aggregates in NR are much weaker than those of oligopeptides functionalized samples, suggesting a less robust network under cyclic loadings.

Effect of Oligopeptides on Thermogenesis and Anti-fatigue Property

In practical applications, NR is usually subjected to dynamic loads. Thus, the ability to maintain its mechanical properties under cyclic forces is highly demanded, which is mainly

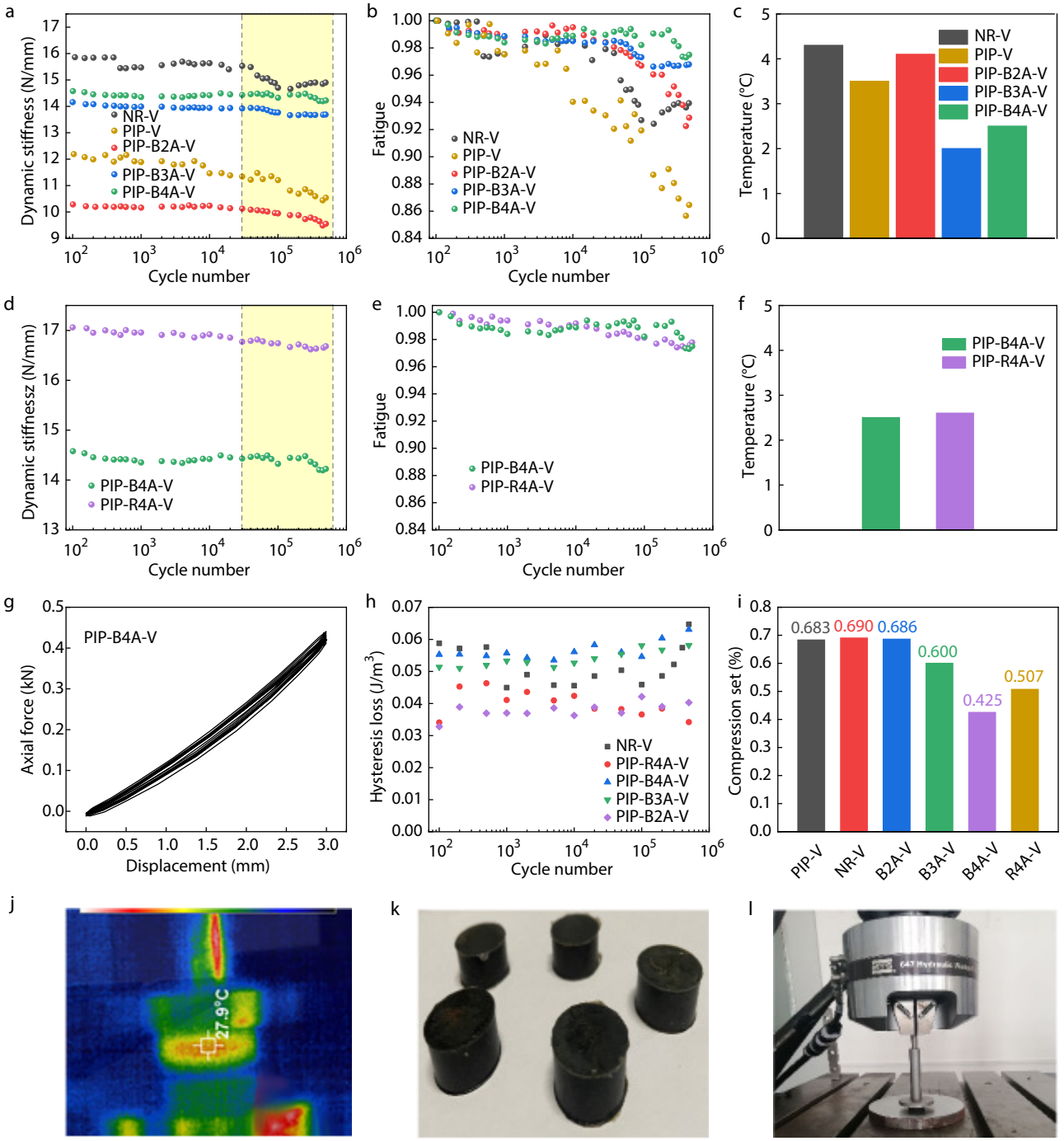

Fig. 5 MTS test results of PIP-V, NR-V and PIP-*X*A-V. (a, d) The variation of dynamic stiffness as the function of cycle numbers; (b, e) The variation of fatigue resistance as the function of cycle number; (c, f) Temperature rising during the MTS test; (g) Stress-strain curves of PIP-B4A-V at selected cycles; (h) Hysteresis loss for each cycle during the MTS test; (i) Compression set; (j) Infrared thermal images at 50W cycles for PIP-V; (k) MTS test samples; (l) MTS test equipment.

https://doi.org/10.1007/s10118-023-2933-3

reflected in anti-fatigue property. Here, we introduce oligopeptides to simulate linked proteins and investigate the effect of hydrogen-bonded aggregates on fatigue resistance and thermogenic properties. The vulcanized cylindrical NR samples were first compressed by 1.5 mm and then subjected to a dynamic force at a displacement of 1.5 mm for 5×10^5 cycles. Figs. 5(a) and 5(d) show the variation of dynamic stiffness (the ability of the rubber to resist deformation under dynamic load) of NR-V, PIP-V and PIP-*X*A-V with the number of loading cycles. It can be seen that dynamic stiffness increases with the elongation of oligopeptide, in which PIP-4A-V has similar dynamic stiffness with NR-V. While PIP-R4A-V has much higher dynamic stiffness, which are ascribed to the enhanced moduli brought by oligopeptide aggregates. For a better comparison, the fatigue resistance can be deduced by dividing the dynamic stiffness in the cyclic test by the initial value. Figs. 5(b) and 5(e) show that all oligopeptide functionalized samples demonstrate similar or superior fatigue resistance relative to NR-V, much higher than those of PIP-V. Among them, PIP-4A-V can maintain above 97% of initial dynamic stiffness even after half a million of cycles, and their fatigue resistances are much better than that of NR-V.

Based on the above results, it is assumed that hydrogen bonding network formed by the oligopeptide play an important role in the cyclic loading. The hysteresis loss of each compression cycle during the MTS tests is tracked and typical values are presented in Fig. 5(h). During half a million of compression cycles, the hystereses of block samples PIP-B*X*A-V keep constant or rise, indicating that the sacrificial bonds not only maintain after the cyclic loading, but also the ordering of hydrogen bonding aggregates rises, forming more robust sacrificial bonds, which is very rare. In contrast, the hysteresis of NR-V first decreases and then increases, indicating that the sacrificial bonds in NR are restorative during the cycling process. However, due to the lack of tight β-sheet structure in NR, the partial destruction of vulcanization network may happen during the earlier cyclic loadings, which will damage the dynamic stiffness. While for PIP-R4A-V, the hysteresis first increases and then drop, indicating a reorganization process of oligopeptide aggregates. Since the hysteresis values are all above the initial value during the compression period, the fatigue resistance is not affected. Meanwhile, For PIP-V sample without any sacrificial bonds, the dynamic stiffness dropped fastest compared to all other samples, demonstrating the critical effects of sacrificial bonds on fatigue resistance.

The dynamic heat generation is also a critical aspect that affect the fatigue life of rubbers. Here we monitor the temperature variations of NR-V, PIP-V and PIP-*X*A-V during 50×10^5 cycles of the MTS experiment (Fig. S16 in ESI). The exact temperature risings of all samples were calculated during the MTS test and the results are compared in Figs. 5(c) and 5(f). It is generally believed that the reversible dissociation/recombination properties of sacrificial bonds lead to increased hysteresis under dynamic forces and increased heat generation, which reduces fatigue life. However, herein PIP-B4A has similar compression cycle hysteresis with NR (Fig. 5h), it demonstrates much lower heat generation and much better fatigue resistance than NR. This breaks the conventional perception of sacrificial bonds on heat generation. It is also found from the stress-strain curves under cyclic compression (Fig. 5g and Fig. S17 in ESI) that the hysteresis circles of PIP-4A-V almost completely overlap, while the hysteresis circles of NR-V and PIP-2A-V are less repetitive, which indicates that PIP-4A-V is more elastic. This will help reduce the thermal accumulation under dynamic loading, which is consistent with the heat generation.

Overall, PIP-4A-V has superior elasticity than NR-V and therefore has better heat generation and fatigue resistance properties, even though it possesses greater hysteresis. Hydrogen-bonded aggregates formed from tetrapeptides have reproducible energy dissipation properties and cyclic lifetimes comparable to or better than that of linked proteins in NR. Moreover, it can be seen that the moderate number of oligopeptides (similar to the content of linked proteins in NR) does not increase the hysteresis heat generation of the rubber.

CONCLUSIONS

In order to make reliable and secure rubber products, we proposed a novel design strategy of adjusting the hydrogen bonding interactions strength and position before vulcanization, which is accomplished *via* oligopeptides self-assembly. The results show that the introduced oligopeptide can form loose and tight *d*-spacing structures simultaneously, which could be break and reform reversibly under cyclic loading. These oligopeptide aggregates not only effectively promote the mechanical properties, but also bring superior fatigue resistance properties. Comparably, the PIP-V sample without sacrificial bonds showed weakest mechanical strength and worst fatigue resistance. NR possesses sacrificial bonds and promote its mechanical property, but the fatigue resistance is inferior to oligopeptide decorated samples due to lack of tight β-sheet structure. Therefore, the hydrogen bond network formed by oligopeptide developed here not only mimic the pseudo-network formed by the linked protein in NR, but also present a more advanced technology to promote the comprehensive properties of polyisoprene rubbers.

Conflict of Interests

The authors declare no interest conflict.

Electronic Supplementary Information

Electronic supplementary information (ESI) is available free of charge in the online version of this article at http://doi.org/10.1007/s10118-023-2933-3.

ACKNOWLEDGMENTS

This work was financially supported by the National Natural Science Foundation of China (No. 51973126) and the State Key Laboratory of Polymer Materials Engineering (No. sklpme2022-2-11).

REFERENCES

1 van Beilen, J. B.; Poirier, Y. Guayule and Russian dandelion as

alternative sources of natural rubber. *Crit. Rev. Biotechnol.* **2007**, *27*, 217–31.
2 Tosaka, M.; Murakami, S.; Poompradub, S.; Kohjiya, S.; Ikeda, Y.; Toki, S.; Sics, I.; Hsiao, B. S. Orientation and crystallization of natural rubber network as revealed by WAXD using synchrotron radiation. *Macromolecules* **2004**, *37*, 3299–3309.
3 Kushner, A. M.; Gabuchian, V.; Johnson, E. G.; Guan, Z. Biomimetic design of reversibly unfolding cross-linker to enhance mechanical properties of 3D network polymers. *J. Am. Chem. Soc.* **2007**, *129*, 14110–14111.
4 Tang, Z.; Huang, J.; Guo, B.; Zhang, L.; Liu, F. Bioinspired engineering of sacrificial metal-ligand bonds into elastomers with supramechanical performance and adaptive recovery. *Macromolecules* **2016**, *49*, 1781–1789.
5 Mareliati, M.; Tadiello, L.; Guerra, S.; Giannini, L.; Schrettl, S.; Weder, C. Metal-ligand complexes as dynamic sacrificial bonds in elastic polymers. *Macromolecules* **2022**, *55*, 5164–5175.
6 Smith, B. L.; Schäffer, T. E.; Viani, M.; Thompson, J. B.; Frederick, N. A.; Kindt, J.; Belcher, A.; Stucky, G. D.; Morse, D. E.; Hansma, P. K. Molecular mechanistic origin of the toughness of natural adhesives, fibres and composites. *Nature* **1999**, *399*, 761–763.
7 Gold, B. J.; Hövelmann, C. H.; Weiss, C.; Radulescu, A.; Allgaier, J.; Pyckhout-Hintzen, W.; Wischnewski, A.; Richter, D. Sacrificial bonds enhance toughness of dual polybutadiene networks. *Polymer* **2016**, *87*, 123–128.
8 Liu, J.; Liu, J.; Wang, S.; Huang, J.; Wu, S.; Tang, Z.; Guo, B.; Zhang, L. An advanced elastomer with an unprecedented combination of excellent mechanical properties and high self-healing capability. *J. Mater. Chem. A* **2017**, *5*, 25660–25671.
9 Bevilacqua, E. Structure of natural rubber. *J. Polym. Sci. Polym. Lett. Ed.* **1967**, *5*, 601–601.
10 Eng, A. H.; Tanaka, Y. *Structure of Natural Rubber*. NIPPON GOMU KYOKAISHI, **1993**.
11 Tanaka, Y. Structural characterization of natural polyisoprenes: solve the mystery of natural rubber based on structural study. *Rubber Chem. Technol.* **2001**, *74*, 355–375.
12 Tarachiwin, L.; Sakdapipanich, J.; Ute, K.; Kitayama, T.; Bamba, T.; Fukusaki, E. I.; Kobayashi, A.; Tanaka, Y. Structural characterization of *α*-terminal group of natural rubber. 1. decomposition of branch-points by lipase and phosphatase treatments. *Biomacromolecules* **2005**, *6*, 1851–1857.
13 Tarachiwin, L.; Sakdapipanich, J.; Ute, K.; Kitayama, T.; Tanaka, Y. Structural characterization of *α*-terminal group of natural rubber. 2. decomposition of branch-points by phospholipase and chemical treatments. *Biomacromolecules* **2005**, *6*, 1858–1863.
14 Toki, S.; Hsiao, B. S.; Amnuaypornsri, S.; Sakdapipanich, J. New insights into the relationship between network structure and strain-induced crystallization in un-vulcanized and vulcanized natural rubber by synchrotron X-ray diffraction. *Polymer* **2009**, *50*, 2142–2148.
15 Toki, S.; Che, J.; Rong, L.; Hsiao, B. S.; Amnuaypornsri, S.; Nimpaiboon, A.; Sakdapipanich, J. Entanglements and networks to strain-induced crystallization and stress-strain relations in natural rubber and synthetic polyisoprene at various temperatures. *Macromolecules* **2013**, *46*, 5238–5248.
16 Amnuaypornsri, S.; Toki, S.; Hsiao, B. S.; Sakdapipanich, J. The effects of endlinking network and entanglement to stress–strain relation and strain-induced crystallization of un-vulcanized and vulcanized natural rubber. *Polymer* **2012**, *53*, 3325–3330.
17 Amnuaypornsri, S.; Sakdapipanich, J.; Toki, S.; Hsiao, B. S.; Ichikawa, N.; Tanaka, Y. Strain-induced crystallization of natural rubber: effect of proteins and phospholipids. *Rubber Chem. Technol.* **2008**, *81*, 753–766.
18 Fu, X.; Huang, C.; Zhu, Y.; Huang, G.; Wu, J. Characterizing the naturally occurring sacrificial bond within natural rubber. *Polymer* **2019**, *161*, 41–48.
19 Zhan, Y. H.; Wei, Y. C.; Tian, J. J.; Gao, Y. Y.; Luo, M. C.; Liao, S. Effect of protein on the thermogenesis performance of natural rubber matrix. *Sci. Rep.* **2020**, *10*, 16417.
20 Li, J.; Du, X.; Hashim, S.; Shy, A.; Xu, B. Aromatic-aromatic interactions enable *α*-helix to *β*-sheet transition of peptides to form supramolecular hydrogels. *J. Am. Chem. Soc.* **2017**, *139*, 71–74.
21 Croisier, E.; Liang, S.; Schweizer, T.; Balog, S.; Mionic, M.; Snellings, R.; Cugnoni, J.; Michaud, V.; Frauenrath, H. A toolbox of oligopeptide-modified polymers for tailored elastomers. *Nat. Commun.* **2014**, *5*, 4728.
22 Tang, M.; Zhang, R.; Li, S.; Zeng, J.; Luo, M.; Xu, Y. X.; Huang, G. Towards a supertough thermoplastic polyisoprene elastomer based on a biomimic strategy. *Angew. Chem. Int. Ed.* **2018**, *57*, 15836–15840.
23 You, Z.; Behl, M.; Grage, S. L.; Burck, J.; Zhao, Q.; Ulrich, A. S.; Lendlein, A. Shape-memory effect by sequential coupling of functions over different length scales in an architectured hydrogel. *Biomacromolecules* **2020**, *21*, 680–687.
24 Finkelmann, H.; Happ, M.; Portugal, M.; Ringsdorf, H. Liquid crystalline polymers with biphenyl-moieties as mesogenic group. *Die Makromolekulare Chemie* **1978**, *179*, 2541–2544.
25 Loiseau, N.; Gomis, J. M.; Santolini, J.; Delaforge, M.; André, F. Predicting the conformational states of cyclic tetrapeptides. *Biopolymers* **2003**, *69*, 363–385.
26 Tang, M.; Bai, S. J.; Xu, R.; Zhang, R.; Li, S. Q.; Xu, Y. X. Oligopeptide binding guided by spacer length lead to remarkably strong and stable network of polyisoprene elastomers. *Polymer* **2021**, *233*, 124185.
27 Huang, W.; Krishnaji, S.; Hu, X.; Kaplan, D.; Cebe, P. Heat capacity of spider silk-like block copolymers. *Macromolecules* **2011**, *44*, 5299–5309.
28 Kato, A.; Ikeda, Y.; Kohjiya, S., Carbon black-filled natural rubber composites: physical chemistry and reinforcing mechanism. In *Polymer Composites*, **2012**, Wiley-VCH, pp 515–543.
29 King, D. R.; Okumura, T.; Takahashi, R.; Kurokawa, T.; Gong, J. P. Macroscale double networks: design criteria for optimizing strength and toughness. *ACS Appl. Mater. Interfaces* **2019**, *11*, 35343–35353.
30 Hou, J. B.; Zhang, X. Q.; Wu, D.; Feng, J. F.; Ke, D.; Li, B. J.; Zhang, S. Tough self-healing elastomers based on the host-guest interaction of polycyclodextrin. *ACS Appl. Mater. Interfaces* **2019**, *11*, 12105–12113.

https://doi.org/10.1007/s10118-023-2933-3